

## **STARK EFFECTS ON RIGID ROTOR WAVEFUNCTIONS:**

### **A Quantum Description of Dipolar Rotors Trapped in Electric Fields as Pendulum Oscillators**

Brad Logsdon and Giles Henderson  
Department of Chemistry  
Eastern Illinois University  
Charleston, IL 61920

Undergraduate physical chemistry students are exposed to qualitative descriptions of the Stark effect as a precise means of measuring the electric dipole moment of molecules (1 - 5). The Stark effect has also been a popular example for introducing students in quantum mechanics to the application of perturbation theory (6 - 11). Approximate eigenvalue expressions derived from perturbation theory are frequently employed by authors of spectroscopy texts to calculate energy level diagrams and to understand the details of the splitting and assignments of atomic and molecular spectra (12 - 15). These traditional discussions focus primarily on the effects of an electric field on the energy levels of an atom or molecule and neglect to disclose the effects of the field on rotational wavefunctions, the molecular motion and molecular orientations.

For many years it has been thought (16,17) that it was impractical to orient gas phase molecules with electric fields because their rotational kinetic energies, approximately  $kT$ , are large compared to the potential barrier due to the interaction energy of a rotating dipole with accessible laboratory fields. However, using molecular beam techniques, it is possible to cool gas molecules in supersonic expansions to rotational temperatures of less than 1 K. It has been shown (18,19) that with such dramatic cooling, significant molecular orientation is feasible with electric fields of ordinary magnitude.

We can anticipate the importance of this technology in future experiments and processes designed to investigate or exploit the dependence of chemical reaction on the orientation of reactant molecules.

The quantum mechanical description of how the Stark effect influences molecular dipole orientation is best understood by examining how the quantum probability function of a rotating molecule,  $\psi^* \psi$ , is altered by an applied electric field. Computer graphics are employed in this project to illustrate orientational probabilities obtained from variational wavefunctions. These results will better enable students to correlate the evolution of free rotor eigenstates with harmonic oscillator type (librator) states as well as compare classical and quantum descriptions of a pendulum oscillator.

## Calculations

We wish to consider a linear rigid rotor with a moment of inertia  $I$  and electric moment  $\mu$  interacting with a uniform electric field  $\mathcal{E}$ . The full three-dimensional description of this problem requires two spherical polar angles to describe the orientation of the rotor in our laboratory frame. The corresponding spherical harmonic wave functions of the rigid rotor in the zero-field limit can be correlated with two dimensional librator wavefunctions of an isotropic spherical pendulum oscillator in the high-field limit. The linear  $n$ -particle rotor is characterized by a moment of inertia

$$I = \sum m_i r_i^2$$

Fig 1(a) illustrates a diatomic rotating about its center of mass.  $m_1$  and  $m_2$  track about circular paths of radii  $r_1$  and  $r_2$  respectively. This 2-particle system is inertially equivalent to the simpler single *particle in a circle*, Fig 1(b), in which

$$I = \mu R^2$$

where  $\mu = m_1 \cdot m_2 / (m_1 + m_2)$  is the reduced mass and  $R = r_1 + r_2$  is the bond length.

### Rotation Restricted to a Plane

Strong electric fields can trap the dipolar molecule as a *Stark pendulum*, Fig 1(c) which undergoes librator motion analogous to an inertial pendulum in a gravity field, Fig 1(d). It greatly simplifies the desired calculations to restrict the rotation to a plane in which the orientation of the rotor is specified by a single angle  $\phi$  (Fig. 1). Moreover, this constraint allows students to better relate the zero-to-high field correlation to their previous experience with one dimensional harmonic oscillators. In the absence of an electric field, we then have the familiar free rotor problem (9) in which the allowed

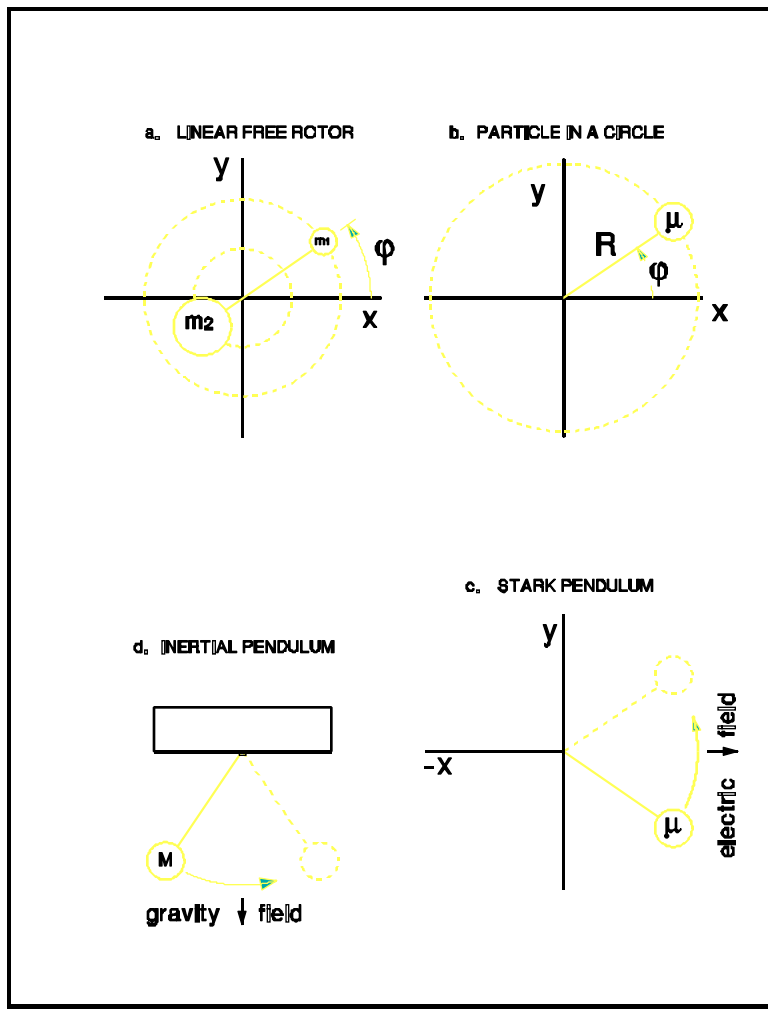


**Figure 1.** The 2-particle rotor (a) is inertially equivalent to a single reduced mass,  $\mu$ , *particle in a circle*, (b). Strong electric fields can trap the dipolar molecule as a *Stark pendulum*, (c) which undergoes librator motion analogous to an inertial pendulum in a gravity field, (d).

kinetic energies of the rotor are given as eigenvalues to the zero order Hamiltonian:

$$\hat{H}_0 \Phi_m = \frac{-\hbar^2}{2I} \frac{d^2}{d\phi^2} \Phi_m(\phi) = E_m \Phi_m(\phi) \quad (1)$$

where  $\hbar$  is Planck's constant divided by  $2\pi$ . The eigenfunctions are simple complex plane waves:

$$\Phi_m(\phi) = \frac{1}{\sqrt{2\pi}} \exp(im\phi) \quad (2)$$

characterized by a quantum number  $m = 0, \pm 1, \pm 2 \dots$ , whose sign designates the direction of rotation, and the allowed energy levels are given by the eigenvalues:  $E_m = m^2 \hbar^2 / (2I)$ .

The rotor experiences an orienting torque if its dipole moment interacts with a uniform electric field,  $\mathcal{E}$ . This interaction results in a potential energy, which hinders the rotational motion and if sufficiently large, can trap the rotor in a bound librator state. This interaction is now included in the Hamiltonian:

$$\hat{H} = \hat{H}_0 + \hat{H}_1 = \frac{-\hbar^2 d^2}{2I d\phi^2} - \mu\mathcal{E} \cos(\phi) \quad (3)$$

Since we will be interested in circumstances where  $\hat{H}_1$  is *not* small compared with  $\hat{H}_0$  we will now employ the variational method with exact matrix diagonalization rather than perturbation theory to find the eigenfunctions and eigenvalues of this operator. In order to construct the matrix representation of eq (3) we shall need integrals of the type:

$$\begin{aligned} \langle m | \hat{H}_1 | m' \rangle &= \int_0^{2\pi} \Phi_m^* \hat{H}_1 \Phi_m d\phi = -\mu\mathcal{E} \int_0^{2\pi} \Phi_m^* \cos(\phi) \Phi_m d\phi \\ &= \frac{-\mu\mathcal{E}}{4\pi} \int_0^{2\pi} \exp(-im\phi) [\exp(i\phi) + \exp(-i\phi)] \exp(im'\phi) d\phi \end{aligned}$$

$$\begin{aligned}
&= \frac{-\mu\mathcal{E}}{4\pi} \int_0^{2\pi} \mathbf{exp}[i\phi(-m+1+m')] d\phi + \frac{-\mu\mathcal{E}}{4\pi} \int_0^{2\pi} \mathbf{exp}[i\phi(-m-1+m')] d\phi \\
&= -\mu\mathcal{E}/2 \text{ for } m' = m \pm 1; \text{ and } 0 \text{ for } m' \neq m \pm 1.
\end{aligned} \tag{4}$$

The Hamiltonian matrix will then have the elements:

$$\langle m | \hat{H} | m \rangle = m^2 \hbar^2 / (2I) = m^2 B \tag{5}$$

$$\langle m | \hat{H} | m \pm 1 \rangle = -\mu\mathcal{E}/2 \tag{6}$$

It is convenient to construct this matrix in units of the rotational constant  $B = \hbar^2 / (2I)$ . The eigenvalues are obtained by diagonalizing the Hamiltonian matrix (20)

$$\mathbf{E} = \mathbf{H}\Psi = \mathbf{a}^\dagger \mathbf{H}^\Phi \mathbf{a} \tag{7}$$

and the wavefunction for each eigenstate is specified in terms of the original orthogonal basis  $\Phi$  by the corresponding eigenvector,  $\Psi = \Phi \mathbf{a}$  or

$$\begin{aligned}
\psi_j &= \sum_m a_{mj} \phi_m = \frac{1}{\sqrt{2\pi}} \sum_m a_{mj} \mathbf{exp}(im\phi) \\
&= \frac{1}{\sqrt{2\pi}} \sum_m a_{mj} \mathbf{cos}(m\phi) + \frac{i}{\sqrt{2\pi}} \sum_m a_{mj} \mathbf{sin}(m\phi)
\end{aligned} \tag{8}$$

Now that the wavefunction for each state is known, we can easily calculate the orientations probability

function:

$$\mathcal{P}_j(\phi) = \psi_j^* \psi_j = \frac{1}{\sqrt{2\pi}} \left[ \sum_m \alpha_{mj} \cos(m\phi) \right]^2 + \frac{1}{\sqrt{2\pi}} \left[ \sum_m \alpha_{mj} \sin(m\phi) \right]^2 \quad (9)$$

Using eq (5) and (6), computer codes are easily written to set up the Hamiltonian matrix for a given Stark interaction energy. The size of the free rotor basis set and the order of  $\mathbf{H}^\Phi$  will depend on the magnitude of the Stark interaction and the desired precision. A basis set of  $0 \leq m \leq \pm 13$  will provide 1 ppm precision for the five lowest eigenstates with Stark energies  $0.0 \leq \mu \mathcal{E} \leq 4B$ . Standard subroutines (21) can be employed to diagonalize  $\mathbf{H}^\Phi$  to obtain the energy eigenvalues and the eigenvectors of the  $\alpha_{mj}$  coefficients of eq (8). The  $\alpha_{mj}$  coefficients for a given  $j$ -eigenstate are used in a loop designed to sweep through the  $\phi$ -domain and evaluate the position probability at each orientation as prescribed by eq (9). This procedure can be nested inside an external loop which systematically increments the Stark interaction. The calculated  $\mathcal{P}(\phi)$  values are then written to disk files for subsequent plotting.

## Results and Discussion

The effect of the Stark field on a free rotors energy levels can be seen in Fig. (2). At the zero-field limit we observe a pattern with familiar second order  $m$ -dependence. The two fold degeneracies associated with  $\pm m$  correspond to clockwise and counter-clockwise rotations of the same energy. As the electric field is

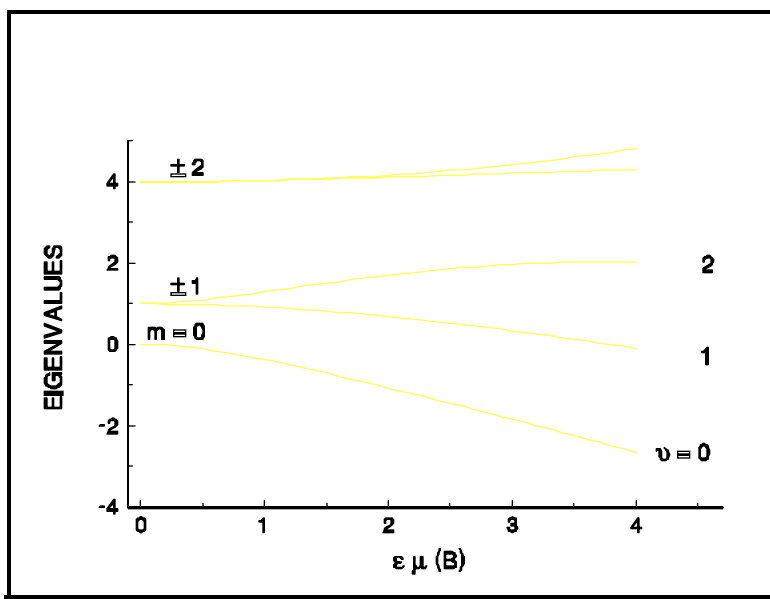


**Figure 2.** The interaction of a molecular dipole with a uniform electric field results in a shifting and splitting of the rotors degenerate energy levels (Stark effect).

turned on we note the m-degeneracy is broken and as the field increases, the lower lying energies began to assume harmonic pendulum oscillator (librator) type spacings:  $1/2 \text{ } h\nu$ ;  $3/2 \text{ } h\nu$ ;  $5/2 \text{ } h\nu \dots$ . These lower lying levels are trapped by the interaction of the rotating dipole moment with the applied electric field as is evident for a Stark interaction  $\mu\mathcal{E} = 4B$  in Fig. (3).

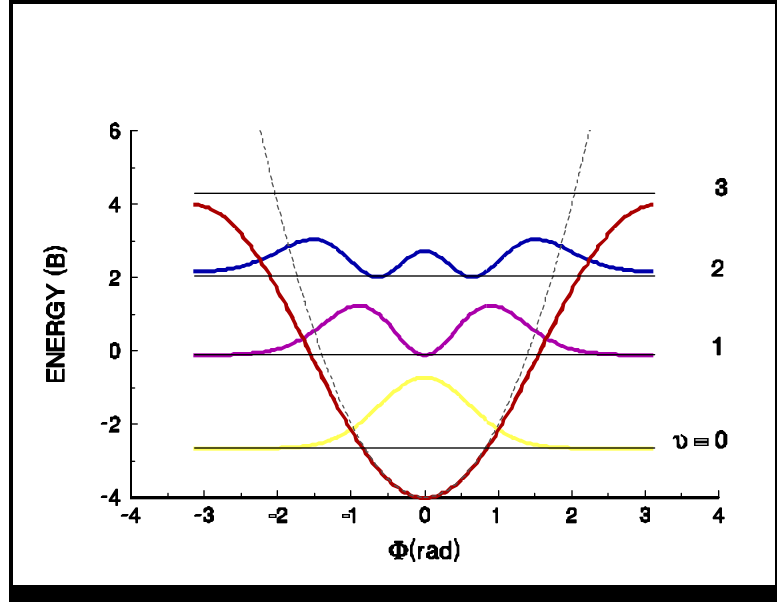


**Figure 3.** The lowest lying energy levels are described by a near harmonic librator in which the rotor is trapped by the Stark field and undergoes pendulum like motions.

The potential energy for this interaction is characterized by a  $\cos(\phi)$  dependence on the dipole orientation, eq (3). If we expand this potential in a power series:

$$-\mu\mathcal{E}\cos(\phi) = -\mu\mathcal{E} + \frac{\mu\mathcal{E}}{2!} \phi^2 - \frac{\mu\mathcal{E}}{4!} \phi^4 \dots \quad (10)$$

we note that for small  $\phi$ , the potential is harmonic with a torque constant  $k\tau = \mu\mathcal{E}$ . The dashed curve in Fig. (3) allows us to compare this harmonic librator potential with the actual Stark potential. Given this description, we can anticipate that the corresponding wavefunctions for these lower levels must began to assume the character of the familiar harmonic oscillator (librator). We can also anticipate that these new wavefunctions will be composed of a mixture of  $\pm m$  basis functions since the trapped rotor spends half of its time rotating clockwise and the other half of its time rotating counter-clockwise as it

librates about its center of mass. This feature is evident in the ground state eigenvector given in Table 1 for  $V = 4B$ .

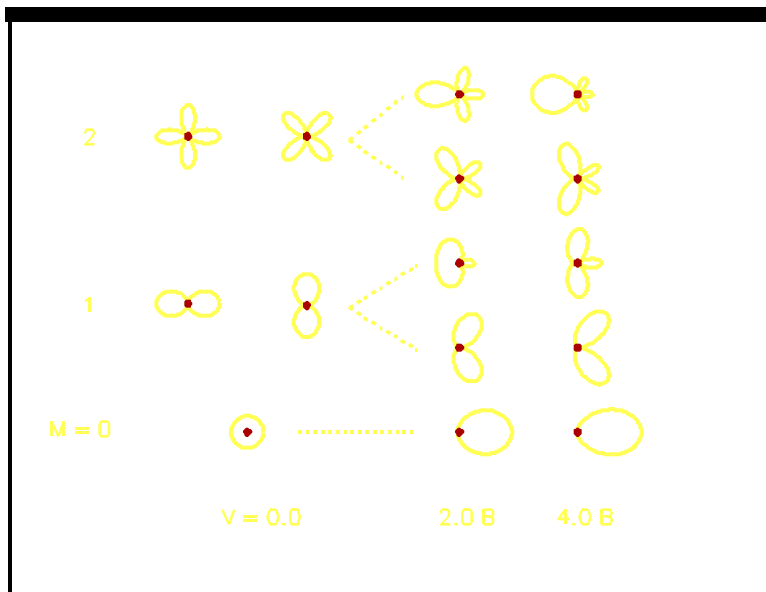
**Table 1.  $V = 4B$  eigenvector for the  $u = 0$  ground state libration.**

$i$	$a_{i,0}$
0	0.712436
1	0.472288
-1	0.472288
2	0.149888
-2	0.149888
3	0.026214
-3	0.026214
4	0.002833
-4	0.002833
5	0.000206
-5	0.000206
6	0.000011
-6	0.000011

We now wish to examine how the free rotor wavefunctions evolve into nearly harmonic libration wavefunctions as the electric field is increased. Polar plots of the wavefunctions of the first 5 states are depicted in Fig. (4) for interaction energies  $V = \mu\mathcal{E} = 0.0, 2.0 B$  and  $4.0 B$ . When the electric field is off ( $V = 0.0$ ) the quantum description of the  $m = 0$  ground state rotor provides an exact value of the angular momentum:  $L = m\hbar = 0$ . However all orientations are equally probable. As the field is

increased, the probability of the dipole being oriented in the direction of the laboratory field ( $\phi = 0.0$ ) is dramatically increased at the expense of other orientations. This new distribution characterizes the small amplitude zero-point motion of the ground state ( $v = 0$ ) librator. The orientational probability function of the higher lying  $V = 4B$  excited maxima at progressively larger  $\pm\phi$  values. The transformations induced

**Figure 4.** Polar plots of  $\psi^*\psi$  at various Stark fields. The zero-field rotor exhibits familiar circular harmonic wavefunctions and  $\pm m$  degeneracies. The Stark field causes an anisotropy in the angular distributions with maxima consistent with a near harmonic liblator.



in these angular functions by the laboratory field are indeed similar to the corresponding hybridization of atomic orbitals induced by the fields of a bonding neighboring atom. Although these functions assume harmonic liblator qualities, students may find this feature may be disguised in the polar space.  $\psi^*\psi$  plots for the lower lying states are compared in both polar and Cartesian space in Fig. 5. It is evident from Fig. 3 that these energy levels are below the Stark potential barrier. Classically, the respective rotors behave as librators with turning points given by:

$$\phi^* = \arccos\left(\frac{E}{-\mu\mathcal{E}}\right) \quad (11)$$

The classical turning point angles are depicted in Fig. 5 as dashed lines. Since the liblator spends most

of its time at  $\phi = \pm\phi^*$ , these angles have the maximum classical orientational probability. It is instructive to note that  $P_v(\phi)$ , the quantum probability functions, also exhibit maxima at similar  $\phi$ -values.

Since  $P_v(\phi)$  is a function of the Stark interaction, these functions can be plotted as surfaces in the  $(\phi, V)$  space. These plots (Fig. 6) allow us to observe the free rotor ( $V = 0.0$ ) functions evolve into approximate harmonic librator functions as the Stark

field is increased. In the absence of a Stark field the  $m > 0$  levels are two-fold degenerate. Therefore any linear combination of the corresponding eigenfunctions (eq 2) are also solutions to the Schrödinger equation. In this study, it is convenient to choose Euler combinations:  $\psi'_+ = \psi_{+m} + \psi_{-m}$  and  $\psi'_- = \psi_{+m} - \psi_{-m}$  in order that these functions can be conveniently correlated with the  $V > 0$  eigenstates of Fig. 3 and 5.

The graphics and computational methods described here can provide students with a better understanding of how quantum mechanics describes the effects of an electric field on a dipolar rotor. Moreover, these descriptions suggest (18) that it is possible to orient rotationally cold molecules produced by supersonic expansions in a molecular beam. These circumstances will undoubtedly be exploited to control the orientation of polar molecules colliding with neutral atoms or nonpolar

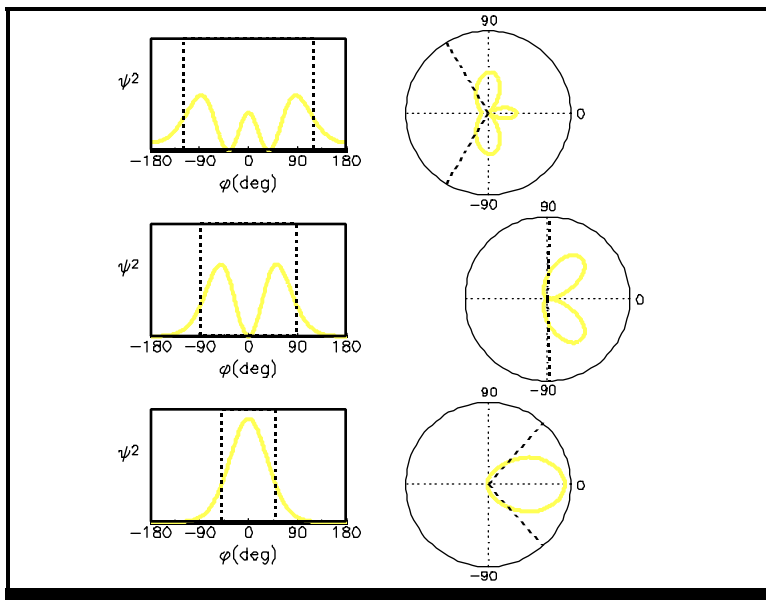


**Figure 5.** The  $\psi^2$  function can be viewed in either a polar or Cartesian space. This correlation allows the student to recognize the expected near harmonic libration character which might otherwise be obscured in the less familiar polar plots. Classical turning points, given in both sets of figures as dashed lines, may be compared with  $\psi^2$  maxima.

molecules. In addition, spectroscopy and electron diffraction studies might also be carried out on oriented gas phase molecules rather than the usual random orientations of a static gas.

### Acknowledgement

The authors wishes to express their gratitude to Scott Martin for pointing out the recent work by B. Friedrich and Professor D. R. Herschbach (19) in this area.

### Literature Cited

1. Adamson, A. W. *A Textbook of Physical Chemistry*, 3rd ed.; Academic Press: New York, 1986; p 829.
2. Levine, I. *Physical Chemistry*, 2nd ed.; McGraw-Hill: New York, 1983; p 700.
3. Moore, W. J. *Physical Chemistry*, 4th ed.; Prentice-Hall: Englewood Cliffs, NJ, 1972, p 761.
4. Noggle, J. H. *Physical Chemistry*, 2nd ed.; Scott and Foresman: Glenview, IL, 1989, p 748,

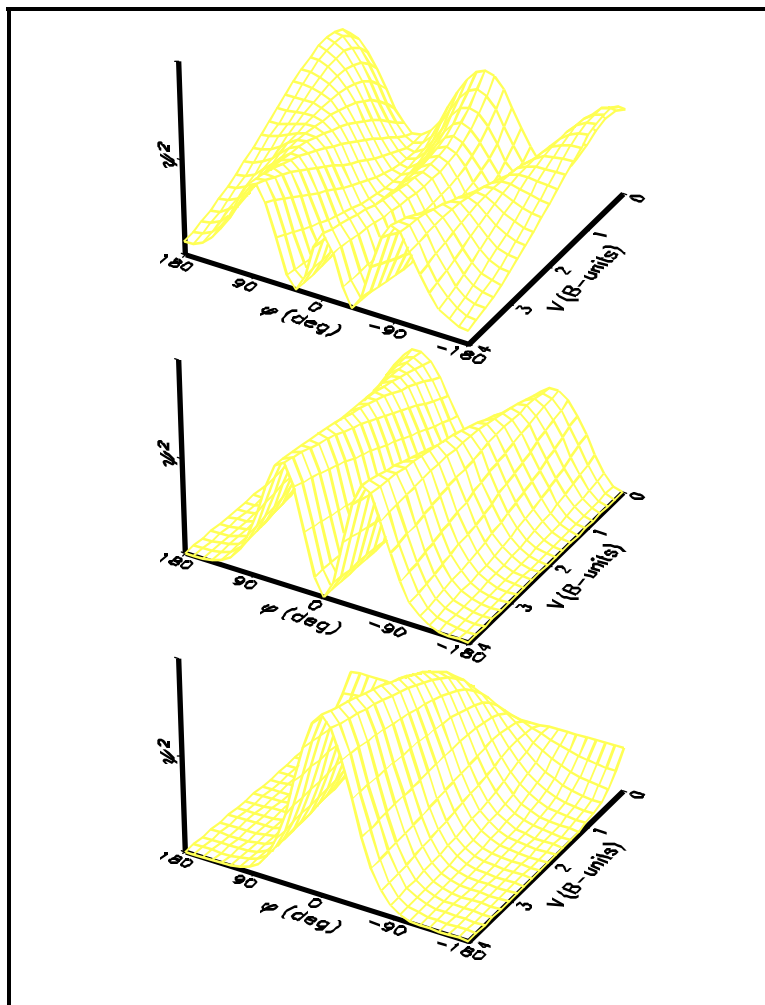


**Figure 6.** The evolution of  $\psi^* \psi$  spherical harmonics of the free rotor to near harmonic librator functions with increasing an increasing Stark field can be easily visualized on a Cartesian surface.

822.

5. Vemulapalli, G. K. *Physical Chemistry*; Prentice-Hall: Englewood Cliffs, NJ, 1993, p 423.
6. Atkins, P. W. *Molecular Quantum Mechanics*, 2nd ed.; Oxford University: Oxford, 1983, p 246.
7. Dykstra, C. E. *Quantum Chemistry and Molecular Spectroscopy*; Prentice-Hall: Englewood Cliffs, NJ, 1992, p 386.
8. Flygare, W. H. *Molecular Structure and Dynamics*; Prentice-Hall: Englewood Cliffs, NJ, 1978, p 191.
9. Pauling, L.; Wilson, E. B. *Introduction to Quantum Mechanics*; McGraw-Hill: New York, 1935, p 177.
10. Schiff, L. I. *Quantum Mechanics*; McGraw-Hill: New York, 1955, p 252, 263.
11. Ref. 5, p 496.
12. Barrow, G. M. *Introduction to Molecular Spectroscopy*; McGraw-Hill: New York, 1962, p 89.
13. Graybeal, J. D. *Molecular Spectroscopy*; McGraw-Hill: New York, 1988, p 386.
14. Guillory, W. A. *Introduction to Molecular Spectroscopy*; Allyn and Bacon: Boston, 1972, p 79, 117.
15. Steinfeld, J. I. *Molecules and Radiation*; Harper and Row: New York, 1974, p 54, 145.
16. Brooks, P. R.; Jones, E. M. *J. Chem. Phys.* **1969**, 51, 3073.
17. Bernstein, R. B.; Herschbach, D. R.; Levine, R. D. *J. Phys. Chem.* **1987**, 91, 5365.
18. Friedrich, B.; Herschbach, D. R. *Z. Phys. D.* **1991**, 18, 153-161.
19. Friedrich, B.; Herschbach, D. R. *J. Phys. Chem.* **1991**, 95, 8118-8129.
20. Ref. 8, p 98.
21. Algorithms for matrix diagonalization are well known. Explicit FORTRAN code for the Jacobi method is given by: Johnson, K. J. *Numerical Methods in Chemistry*; Marcel Dekker: New York, 1980, pp 407-429.